J Nanostruct 16(3): 3346-3356, Summer 2026

RESEARCH PAPER

Green Production of Silver Nanoparticle Using Mushroom Extract Against Leishmania *in vivo*

Hawraa H. Esmael

Clinical laboratory science branch, College of Pharmacy, Al- Nahrain University, Baghdad, Iraq

ARTICLE INFO

Article History:
Received 10 March 2026
Accepted 16 May 2026
Published 01 July 2026

Keywords:
Agaricus bisporus
Green synthesis
Leishmania donovani
Nanotherapy
Pentostam
Silver nanoparticles

ABSTRACT

The emergence of nanotechnology has enabled novel strategies for treating parasitic infections, particularly through the use of biosynthesized nanoparticles. This study focuses on the green synthesis of silver nanoparticles (AgNPs) using white mushroom (*Agaricus bisporus*) extract as a bioreducing and stabilizing agent and evaluates their therapeutic efficacy against *Leishmania donovani* in a murine model of visceral leishmaniasis (VL). The synthesized AgNPs were characterized using X-ray diffraction (XRD), UV–visible spectroscopy, and scanning electron microscopy (SEM), confirming their spherical morphology, crystalline structure, and surface plasmon resonance at ~430 nm. Mice were divided into five groups: healthy control, infected control, AgNPs-treated, Pentostam-treated, and AgNPs + Pentostam-treated. Treatment with AgNPs, either alone or in combination with Pentostam, significantly reduced liver and spleen enlargement or restored hematological parameters toward normal levels. The combined treatment showed the most notable therapeutic benefit, indicating a synergistic effect. These findings support the potential of mushroom-mediated AgNPs as a biocompatible and effective adjunct therapy for visceral leishmaniasis, offering a sustainable and less toxic alternative to conventional treatments.

How to cite this article
Esmael H. Green Production of Silver Nanoparticle Using Mushroom Extract Against Leishmania in vivo. J Nanostruct, 2026; 16(3):3346-3356. DOI: 10.22052/JNS.2026.03.028

INTRODUCTION

Nanotechnology has emerged as a transformative field, offering innovative solutions across medicine, agriculture, and environmental science. Among various nanomaterial's, silver nanoparticles (AgNPs) have garnered substantial interest due to their well-documented antimicrobial, antiparasitic, and anti-inflammatory properties [1,2]. Traditional chemical and physical methods for synthesizing AgNPs often involve toxic reagents and energy-intensive processes, raising environmental and health concerns. In contrast, green synthesis methods, particularly those utilizing biological organisms such as plants, fungi, and bacteria, offer an eco-friendly and sustainable alternative [3, 4].

Mushrooms, especially edible and medicinal species, have emerged as efficient bioreducing and stabilizing agents in nanoparticle synthesis due to their rich content of bioactive compounds, including polysaccharides, phenolics, flavonoids, and proteins [5]. These biomolecules not only facilitate the reduction of silver ions but also enhance the biocompatibility and stability of the resulting nanoparticles. Furthermore, mushrooms such as *Ganoderma lucidum* and *Pleurotus*

* *Corresponding Author Email: dr.hawraa.hashim@nahrainuniv.edu.iq*

spp. have been successfully used in the green synthesis of AgNPs with potent antimicrobial and antiparasitic activities [6-7].

The application of mushroom-mediated silver nanoparticles in vivo against parasitic infections is a novel and promising strategy. Parasitic diseases remain a significant global health burden, particularly in developing countries, and the rise of drug-resistant strains necessitates the development of alternative therapeutic agents. AgNPs synthesized using mushroom extracts offer a dual advantage: they are less toxic than chemically synthesized nanoparticles and demonstrate effective antiparasitic activity through mechanisms such as membrane disruption, reactive oxygen species (ROS) generation, and interference with metabolic pathways [8].

This study aims to explore the green synthesis of silver nanoparticles using mushroom extracts and evaluate them in vivo efficacy against parasitic infections, contributing to the development of sustainable, biocompatible, and effective nanotherapeutics.

MATERIALS AND METHODS

Chemicals and biological materials

Preparation of white mushroom extraction

Preparation for extracting white mushrooms exclude any organic pollutants, 25 grams of fresh mushrooms were collected and rinsed several times in distilled water. Then, the crushed pieces and 500 mL of distilled water were added to a 1 L beaker and thoroughly agitated for 30 minutes. Finally, the mixture was filtered using Whatman filter paper. Here, the reducing and stabilizing agent for the synthesis of Ag NPs is mushroom extract (Fig. 1).

Cell culture

The *Leishmania donovani* strain (DUAA/IQ/2005/MRU15) was obtained from the Department of Biology, University of Al-Mustansiriya. The parasites were maintained and subcultured weekly in RPMI-1640 medium (Sigma, St. Louis, MO, USA) supplemented with 2 mM L-glutamine, 10% fetal bovine serum (FBS), and 100 µg/mL penicillin. To maintain sterility, the medium was filtered through a 0.22 µm pore-size membrane filter before use. After preparation, the medium was stored at 2–8 °C until use. Cultures were initiated in 5 mL of RPMI-1640 medium with 10% FBS at a density of 1×10^6 cells/mL and incubated at 27 °C in a sterile environment. Sub culturing was performed on a weekly basis to maintain optimal parasite viability and growth [9].

Synthesis of silver nanoparticles

In order to create silver nanoparticles (Ag NPs), 80 mL of 0.306 g silver nitrate ($AgNo_3$) solution and 20 mL of white mushroom extract were combined in 200 mL Erlenmeyer flasks. The reaction was then carried out at 60 C° on a magnetic heating stirrer. The first indication of the creation of silver nanoparticles is the two-hour change in color of

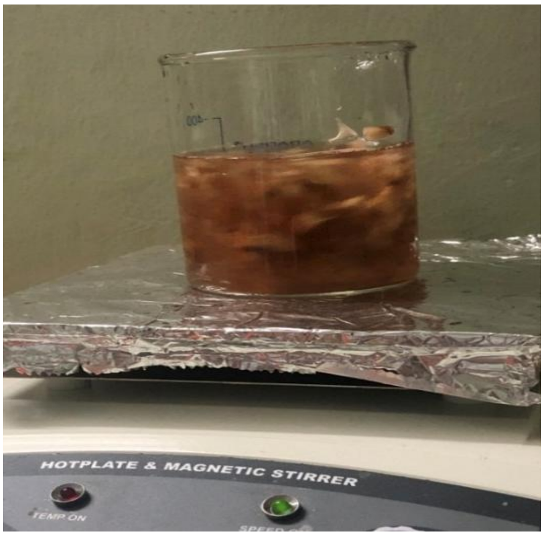

Fig. 1. Mushroom Extract.

the reaction mixture from light yellow to dark brown (Fig. 2).

Following the completion of the silver nanoparticle production process, the finished product was centrifuged for 15 min. at 12.000 rpm. This was done in order to assure the separation of free entities from the silver nanoparticles. The resulting material was made into a powder and dried at room temperature (Fig. 3).

Determination of effects of AgNPs on parasites

AgNPs effectiveness in vivo was evaluated in five groups of mice (6 animals /group) with visceral leishmania (VL). The remaining two groups received peritoneal injections of Sb drug (350 µg/ml) once daily for 28 days whereas two groups received peritoneal injections of Ag NPs (350 µg/ml) once daily for 28 days. Additionally, healthy mice without infection or therapy served as the negative control, whereas a group of VL-infected mice were left untreated (Fig. 4).

Total animals: 30 mice Groups (n=6 each):
Negative control (healthy)
Positive control (infected, untreated)
Infected + AgNPs (350 µg/ml)
Infected + Pentostam (350 µg/ml)
Infected + AgNPs + Pentostam

Measurements

Body weight was recorded before and after treatment. After sacrifice, liver and spleen were

Fig. 2. shown the change light yellow to dark brown.

Fig. 3. The Ag Nps dried at room temperature.

weighed.

Organ-to-body weight ratio was calculated as:

Orange Ratio = Orange Weight (g) / Body Weight (g) × 100

Blood samples were collected to perform CBC analysis (RBC, WBC, Hb, HCT, PLT).

Characterization of Silver Nanoparticles

X-Ray Diffraction Studies (XRD)

X-ray diffraction (XRD) is a powerful analytical technique widely used to determine the crystalline structure, phase identification, crystallite size, and purity of nanoparticles such as silver nanoparticles (AgNPs). Principle of XRD, When X-rays are directed at a crystalline substance, they are diffracted

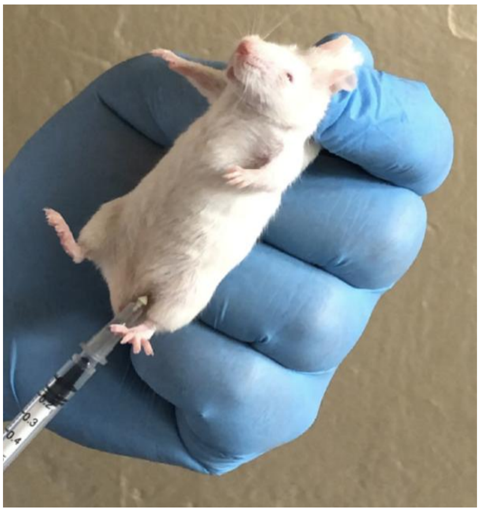

Fig. 4. a. Intra peritoneal Injection of Laboratory Mouse during Experimental Infection, b. Isolated Mouse Liver and Spleen for Organ Weight Assessment.

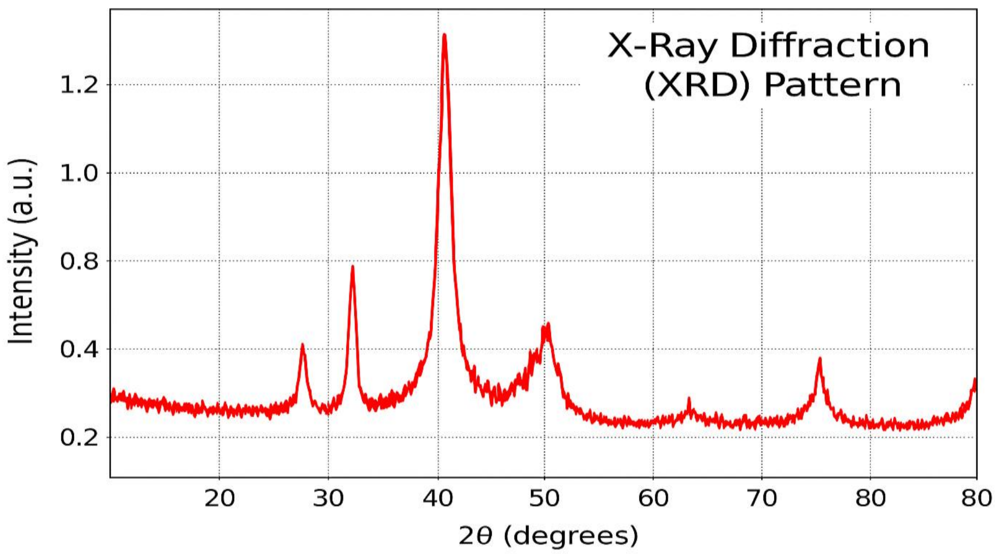

Fig. 5. Patterns of X-ray diffraction for Ag NPs.

in specific directions. The resulting diffraction pattern provides detailed information about the arrangement of atoms within the material. The powder X-ray diffraction of the Ag NPs is shown in Fig. 5, The XRD analysis indicates that the silver nanoparticles exhibit a polycrystalline structure with a cubic phase, which matches the standard diffraction pattern of silver according to the JCPDS card no. 96-901-3049. The obtained results are in good agreement with previous studies [10-11].

The diffraction pattern displays several Bragg reflection peaks corresponding to the (hkl) planes, observed at 2θ values at ap,j proximately 38.1°, 44.3°, 64.4°, and 77.4°, which are indexed to the (111), (200), (220), and (311) planes, respectively, indicating the face-centered cubic (FCC) structure of metallic silver. The average crystallite size was estimated using the Debye–Scherrer formula and found to be ~25 nm, indicating the nanoscale nature of the particles.

FTIR Analysis of Silver Nanoparticles

The FTIR spectrum of the biosynthesized silver nanoparticles shows several characteristic absorption bands that indicate the presence of functional groups involved in the reduction and stabilization of AgNPs:

Broad band at ~3412 cm^{-1}: This is attributed to the O–H stretching vibrations of hydroxyl groups present in phenolic compounds, alcohols, or polysaccharides. These compounds likely act as reducing agents and stabilizers [12]. Peak at ~1640 cm^{-1}: This band corresponds to the C=O stretching vibrations of amide groups or carbonyl compounds, indicating the involvement of proteins or enzymes in nanoparticle synthesis [13]. Peak at ~1382 cm^{-1}: This is associated with C–N stretching of aromatic amines or bending vibrations of $–CH_3$ groups, also related to proteins or other organic compounds in the extract [14]. Peak at ~1106 cm^{-1}: This may correspond to C–O–C or C–O stretching vibrations from polysaccharides or alcohols, supporting their involvement in capping the nanoparticles [15].

The FTIR results confirm the successful capping and stabilization of AgNPs by biomolecules from the fungal extract. Functional groups such as hydroxyl, carbonyl, amide, and amine groups are crucial in reducing silver ions (Ag^+) to elemental silver (Ag^0) and stabilizing the formed nanoparticles (Fig. 6).

UV-Visible spectral

Through visual inspection, silver nanoparticles generate the change in color from light yellow to dark brown (Fig. 7). The variations in excitation energy of the particle surface plasmon resonance could be the cause of the color change. A surface plasmon resonance peak (SPR) at around 430 nm, which is associated with Ag NP synthesis, can be seen in the UV-visible spectrum [11, 12, 16].

Measured in the range of 300–1100 nm. The key observations include:

A strong absorption peak at approximately 430

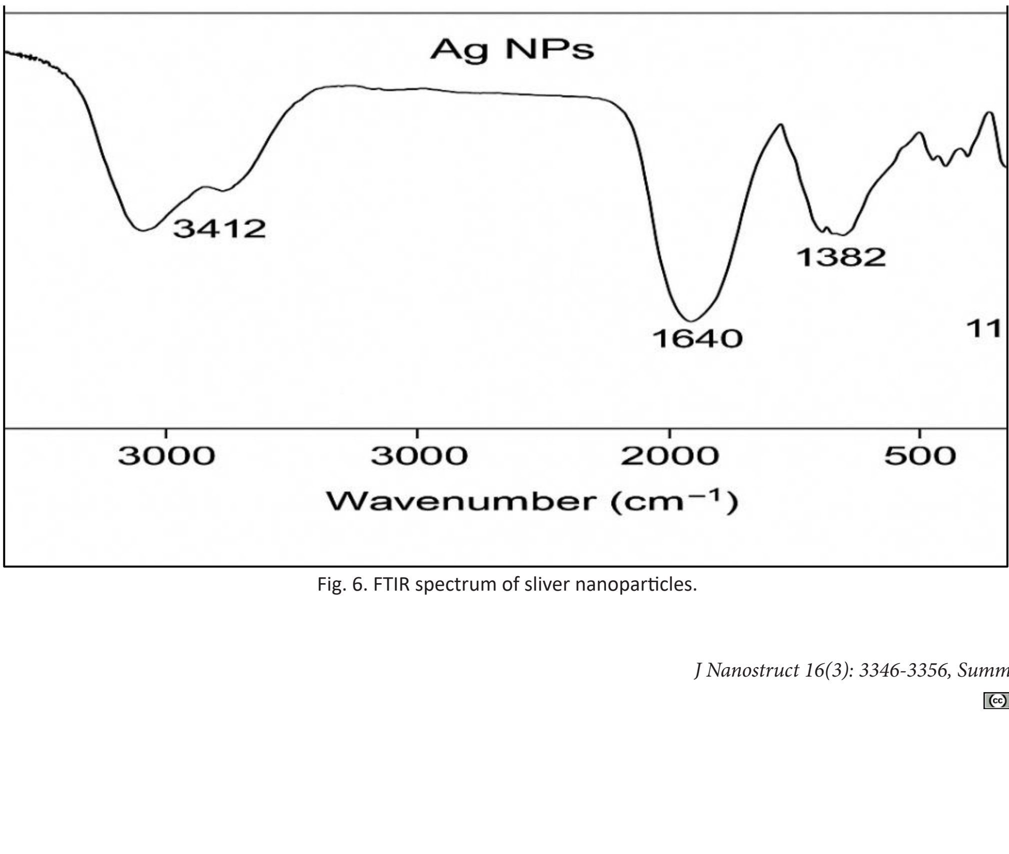

Fig. 6. FTIR spectrum of sliver nanoparticles.

nm, which is characteristic of the surface plasmon resonance (SPR) of AgNPs.

The SPR arises due to the collective oscillation of conduction electrons in response to light, and this peak typically occurs between 400–450 nm for AgNPs, depending on size, shape, and surrounding medium. The broad tail extending toward longer wavelengths (>600 nm) is typical and may indicate polydispersity or aggregation of nanoparticles. These results are a good agreement with study of Kora etal. & Khalil et al [17,18].

Scanning Electron microscopy (SEM)

The surface morphology of the synthesized silver nanoparticles (Ag NPs) was examined using Scanning Electron Microscopy (SEM) (Fig. 8). The results revealed that the Ag NPs were predominantly spherical in shape with sizes ranging from 20 to 40 nm. These nanoparticles appeared as crystalline solid clusters aggregated

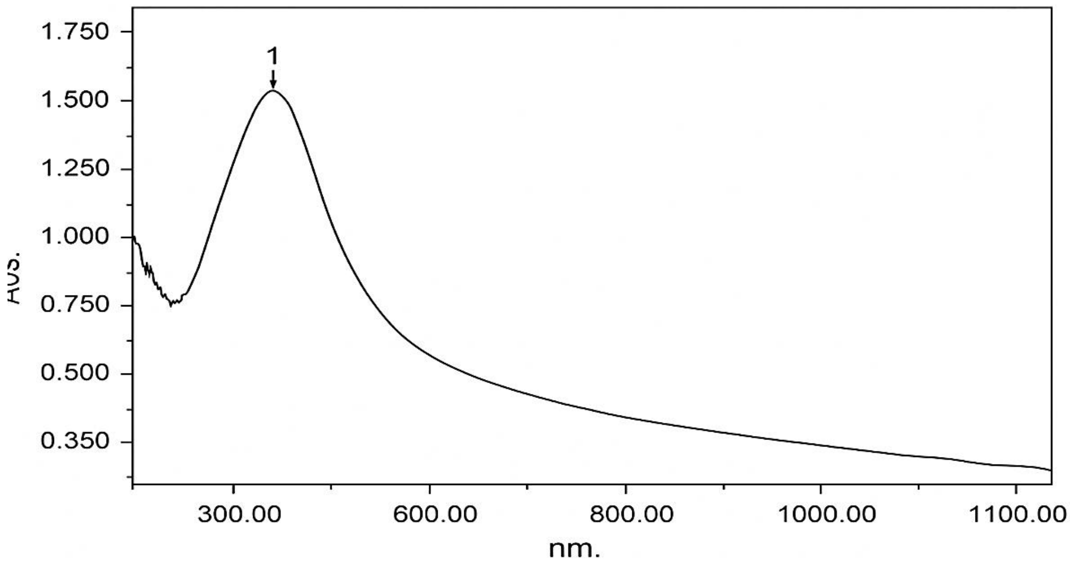

Fig. 7. UV-Vis absorption spectrum of silver nanoparticles (AgNPs).

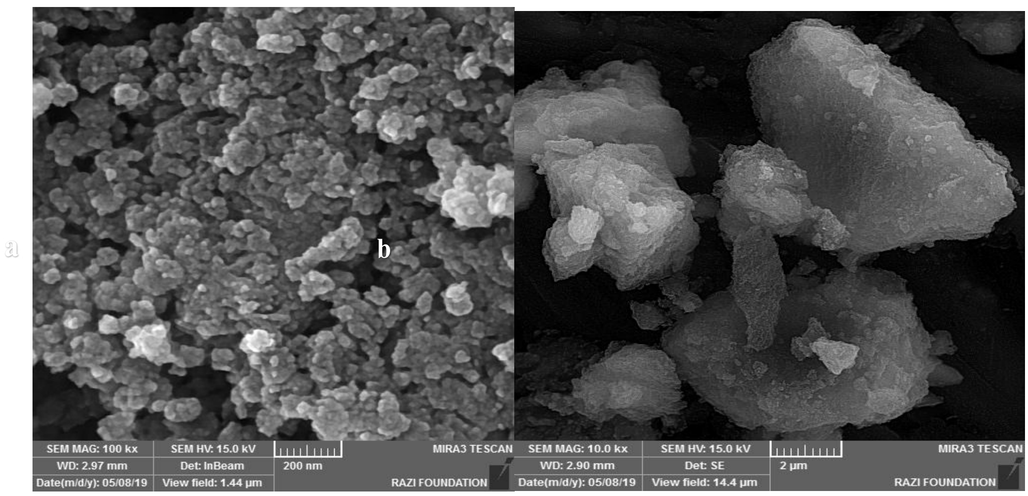

Fig. 8. a. SEM Micrograph of Biosynthesized Silver Nanoparticles Showing Aggregated Spherical Morphology at 100,000× Magnifications b. SEM Micrograph of Aggregated Silver Nanoparticle Clusters at 10,000× Magnification.

into small masses, with individual particles showing diameters less than 50 nm. This morphological feature supports the role of plant extracts as effective reducing and capping agents during green synthesis. The observed results are consistent with several previous studies reporting similar size ranges and morphologies of biosynthesized Ag NPs using plant-mediated approaches [19-21].

RESULTS AND DISCUSSION

The infected control group showed a significant increase in both liver and spleen weights and their respective percentages relative to body weight, indicating organomegaly caused by visceral leishmaniasis.

Treatment with silver nanoparticles (AgNPs), Pentostam, or their combination reduced organ enlargement, with the AgNPs + Pentostam group showing the most marked improvement, approaching normal values.

This bar chart displays the effect of infection and treatment on liver and spleen weights, and their percentages relative to body weight in five groups: Liver Weight and Liver %, Infected Control: Shows a dramatic increase in liver weight and liver % compared to the Healthy Control. This indicates hepatomegaly (liver enlargement), a typical response to visceral *leishmaniasis*. AgNPs, Pentostam, and AgNPs + Pentostam Treated Groups: Liver weight and % decreased significantly after treatment. The AgNPs + Pentostam group showed liver values nearly restored to normal, indicating effective treatment. Spleen Weight and Spleen Infected Control: Also had a marked increase in spleen weight and % indicating splenomegaly, another hallmark of visceral *leishmaniasis*. AgNPs and Pentostam treatments: Caused a partial reduction in spleen size. AgNPs + Pentostam: Caused the most pronounced improvement, almost reaching the healthy control levels.

Table 1. Organ Weights and Ratios in Different Groups.

Group	Body Weight (g)	Liver Weight (g)	Liver %	Spleen Weight (g)	Spleen %
Healthy Control	25.1 ± 1.3	1.22 ± 0.1	4.86%	0.12 ± 0.02	0.48%
Infected Control	23.8 ± 1.0	2.45 ± 0.2	10.29%	0.48 ± 0.03	2.02%
AgNPs Treated	24.7 ± 1.1	1.45 ± 0.15	5.87%	0.22 ± 0.03	0.89%
Pentostam Treated	24.5 ± 1.0	1.67 ± 0.12	6.81%	0.25 ± 0.04	1.02%
AgNPs + Pentostam	25.0 ± 0.9	1.30 ± 0.1	5.2%	0.15 ± 0.02	0.6%

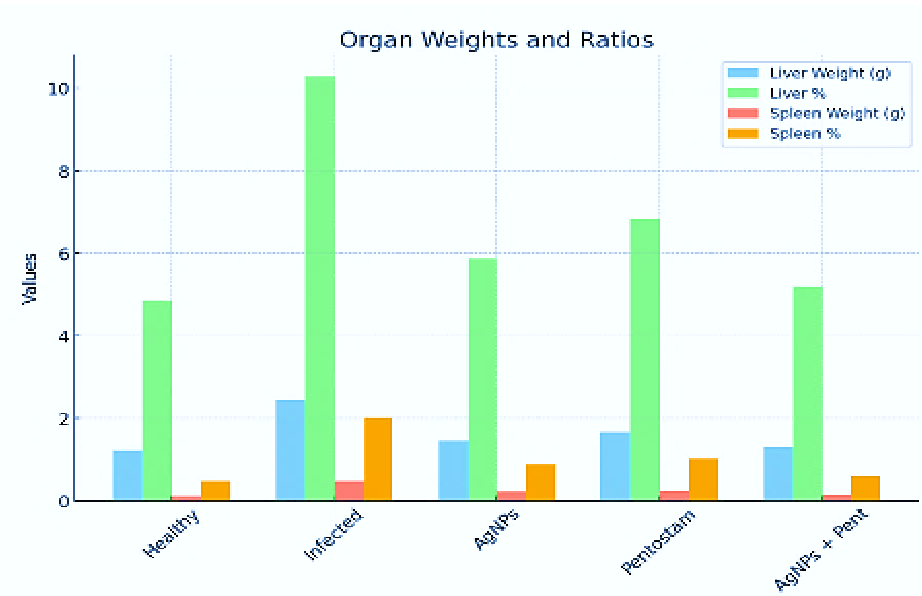

Fig. 9. bar of organ weight and ratio.

Infection led to anemia (decreased RBC, Hb, and HCT) and leukocytosis (elevated WBC), with a notable drop in platelet count (PLT). All treatments significantly improved hematological parameters, especially in the combined AgNPs + Pentostam group, which nearly restored values to those of the healthy control group (Fig. 10).

This bar chart shows how the infection and different treatments affected hematological parameters (RBC, WBC, Hb, HCT, PLT):

RBC (Red Blood Cells), Hb (Hemoglobin), and HCT (Hematocrit)Infected Control: These values are significantly reduced, reflecting anemia due to infection. AgNPs and Pentostam treatments: Each treatment partially improved anemia. AgNPs + Pentostam: Showed the highest improvement, with values close to the healthy group.WBC (White Blood Cells) Infected Control: WBC count is elevated, indicating an immune response (leukocytosis) due to the parasite. All treatment groups: Show a reduction in WBC count, with the combined treatment again being most effective, nearly normalizing the immune response.

PLT (Platelets) Infected Control: Platelet count is significantly reduced, indicating thrombocytopenia, common in *leishmaniasis*. All treatments: Show a gradual recovery in platelet levels, with AgNPs + Pentostam bringing the count close to healthy values.

The results of the present study demonstrate that *Leishmania donovani* infection in mice leads to significant pathological changes, particularly hepatosplenomegaly and hematological abnormalities, which are hallmark features of visceral l*eishmaniasis* (VL). These pathological signs are consistent with previously reported findings that VL primarily targets the liver, spleen, and bone marrow, leading to immune dysregulation and organ damage [22-23].

Table 2. Complete Blood Count (CBC) Results.

Group	RBC ($\times10^6$/µL)	WBC ($\times10^3$/µL)	Hb (g/dL)	HCT (%)	PLT ($\times10^3$/µL)
Healthy Control	8.1 ± 0.3	6.5 ± 0.4	14.2 ± 0.5	42.3 ± 1.2	850 ± 50
Infected Control	5.4 ± 0.2	11.8 ± 0.6	9.1 ± 0.4	30.7 ± 1.0	520 ± 40
AgNPs Treated	7.3 ± 0.3	7.2 ± 0.5	12.7 ± 0.3	39.5 ± 1.1	770 ± 45
Pentostam Treated	7.0 ± 0.4	7.8 ± 0.6	12.3 ± 0.5	38.2 ± 1.4	740 ± 60
AgNPs + Pentostam	7.8 ± 0.2	6.9 ± 0.4	13.5 ± 0.4	41.1 ± 0.9	810 ± 55

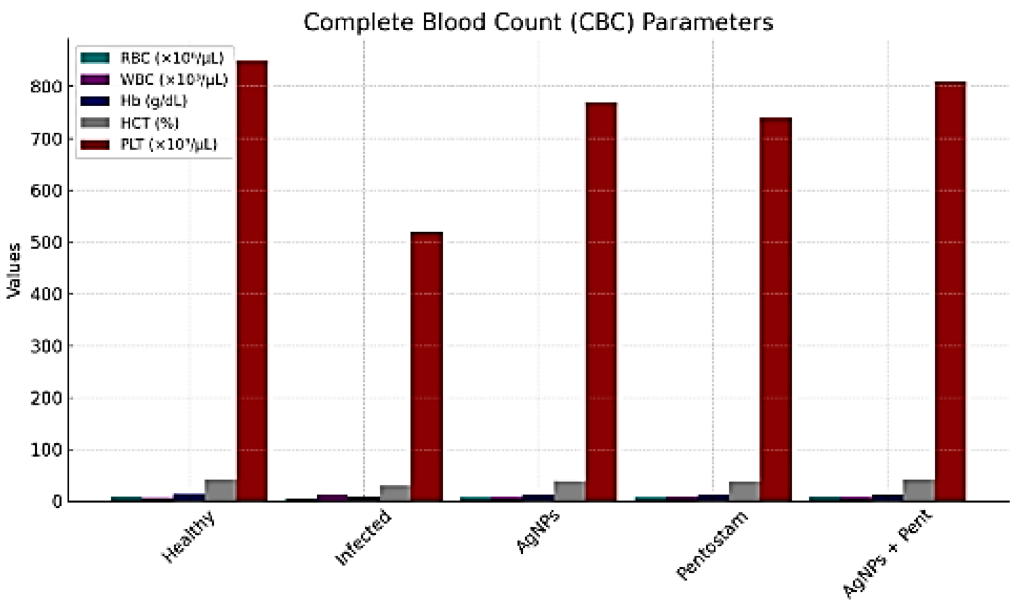

Fig. 10. CBC Parameters Chart.

Organomegaly (Liver and Spleen Changes)

Mice in the infected control group exhibited a significant increase in liver and spleen weights and their respective percentages relative to body weight (Table 1). This hepatosplenomegaly reflects the accumulation of inflammatory cells and parasitized macrophages in these organs, as reported in prior studies [24]. Such enlargement is part of the immune response to parasitic burden and results from hyperplasia of the mononuclear phagocyte system, as previously described by Melby et al. [25].

Following treatment, both AgNPs and Pentostam groups showed a reduction in liver and spleen weights, with the AgNPs + Pentostam combination resulting in near-normal values. These results align with previous findings that Pentostam (sodium stibogluconate), a standard antileishmanial drug, reduces parasite load and inflammatory damage [26].

Additionally, silver nanoparticles (AgNPs) have demonstrated strong antileishmanial properties, likely through multiple mechanisms, including disruption of parasite membranes, generation of reactive oxygen species (ROS), and modulation of host immune responses [27,28]. The synergy observed in the AgNPs + Pentostam group may be due to complementary mechanisms of action with AgNPs enhancing oxidative stress and Pentostam interfering with parasite metabolism.

Hematological Parameters

The CBC data (Table 2) confirm that visceral *leishmaniasis* leads to hematological disturbances, such as: Anemia (decreased RBC, Hb, HCT), Leukocytosis (increased WBC).

Thrombocytopenia (decreased PLT)

These findings reflect bone marrow suppression and splenic sequestration of blood cells during *L. donovani* infection, as documented by Pagliano & Esposito [29] and Dourado[30].

Post-treatment hematological recovery was evident in all treated groups, with the AgNPs + Pentostam group showing the most significant improvement. This supports previous studies where nanoparticles enhanced hematological profiles during parasitic infections due to their immunomodulatory and antioxidant properties [31,32]. The restoration of RBC, Hb, HCT, and PLT levels to near-healthy values further indicates that combination therapy is more effective than monotherapy.

Therapeutic Implications

The results suggest that the combination of AgNPs and Pentostam not only improves parasite clearance, but also helps to preserve hematological integrity and prevent organ damage, likely via synergistic mechanisms. This is consistent with recent research advocating nanoformulations as adjunct therapy to enhance the efficacy of traditional antileishmanial drugs and reduce resistance development [33-35].

CONCLUSION

This study demonstrated the successful green synthesis of silver nanoparticles (AgNPs) using white mushroom extract as a natural reducing and stabilizing agent. The biosynthesized nanoparticles were confirmed and characterized through multiple analytical techniques. XRD analysis revealed a crystalline face-centered cubic (FCC) structure of metallic silver with an average crystallite size of approximately 25 nm. UV–Vis spectroscopy showed a characteristic surface plasmon resonance peak around 430 nm, confirming nanoparticle formation, while FTIR analysis indicated that functional groups such as hydroxyl, carbonyl, and amide groups from mushroom biomolecules played a key role in the reduction and stabilization of AgNPs. SEM observations further showed that the nanoparticles were predominantly spherical with sizes ranging from 20–40 nm. The in vivo evaluation demonstrated that infection with *Leishmania donovani* caused significant pathological changes in mice, including hepatomegaly, splenomegaly, anemia, leukocytosis, and thrombocytopenia. Treatment with AgNPs significantly improved these pathological and hematological parameters, indicating notable antileishmanial activity. Moreover, the combination of AgNPs with Pentostam produced the most pronounced therapeutic effect, reducing liver and spleen enlargement and restoring blood parameters close to normal levels. Overall, the findings highlight that mushroom-mediated silver nanoparticles represent a promising, eco-friendly nanotherapeutic agent with significant antileishmanial potential. Furthermore, their combination with conventional drugs such as Pentostam may enhance treatment efficacy and reduce disease-associated complications, suggesting a valuable strategy for future antiparasitic therapies.

CONFLICT OF INTEREST

The authors declare that there is no conflict of interests regarding the publication of this manuscript.

REFERENCES

1. Rai M, Yadav A, Gade A. Silver nanoparticles as a new generation of antimicrobials. Biotechnol Adv. 2009;27(1):76-83.
2. H. Ismail H, Abdulla Hasoon S, J. Saheb E. The anti-Leishmaniasis activity of green synthesis silver oxide nanoparticles. Africa Health Research Organization. 2019;22(04):28-38.
3. Iravani S, Korbekandi H, Zolfaghari B. Phytosynthesis of Nanoparticles. Nanotechnology and Plant Sciences: Springer International Publishing; 2015. p. 203-258.
4. Int C. Green synthesis, characterization of silver sulfide nanoparticles and antibacterial activity evaluation. Center for Open Science; 2019.
5. Ghodake G, Lim S-R, Lee DS. Casein hydrolytic peptides mediated green synthesis of antibacterial silver nanoparticles. Colloids Surf B Biointerfaces. 2013;108:147-151.
6. Durán N, Marcato PD, De Souza GIH, Alves OL, Esposito E. Antibacterial Effect of Silver Nanoparticles Produced by Fungal Process on Textile Fabrics and Their Effluent Treatment. J Biomed Nanotechnol. 2007;3(2):203-208.
7. Arumugam S, Kasumbwe K, Mohanlall V. Mycosynthesis of silver nanoparticles from Pleurotus ostreatus extracts: antibacterial and catalytic activity evaluation. Braz J Biol. 2025;85.
8. Rojas-Torres L, Furlan LA, Sánchez-Rosas J, Rojas-Rojas G. Escala de Afrontamiento de la Ansiedad durante los Exámenes. PsycTESTS Dataset: American Psychological Association (APA); 2022.
9. In Vitro and In Vivo Anticancer and Genotoxicity Profiles of Green Synthesized and Chemically Synthesized Silver Nanoparticles. American Chemical Society (ACS).
10. Ajibesin KK, Adebayo-Tayo BC. Antimicrobial Activities of Coula edulis. Research Journal of Medicinal Plant. 2008;2(2):86-91.
11. Ahmed S, Ahmad M, Swami BL, Ikram S. A review on plants extract mediated synthesis of silver nanoparticles for antimicrobial applications: A green expertise. Journal of Advanced Research. 2016;7(1):17-28.
12. Singh P, Kim Y-J, Zhang D, Yang D-C. Biological Synthesis of Nanoparticles from Plants and Microorganisms. Trends Biotechnol. 2016;34(7):588-599.
13. Cheera P, Karlapudi S, Sellola G, Ponneri V. A facile green synthesis of spherical Fe3O4 magnetic nanoparticles and their effect on degradation of methylene blue in aqueous solution. J Mol Liq. 2016;221:993-998.
14. Figure 3: FTIR spectra of AgNPs synthesized by bacteria. PeerJ. http://dx.doi.org/10.7717/peerj.17328/fig-3
15. Shahzadi S, Fatima S, ul ain Q, Shafiq Z, Janjua MRSA. A review on green synthesis of silver nanoparticles (SNPs) using plant extracts: a multifaceted approach in photocatalysis, environmental remediation, and biomedicine. RSC Advances. 2025;15(5):3858-3903.
16. Eker F, Akdaşçi E, Duman H, Bechelany M, Karav S. Green Synthesis of Silver Nanoparticles Using Plant Extracts: A Comprehensive Review of Physicochemical Properties and Multifunctional Applications. Int J Mol Sci. 2025;26(13):6222.
17. John Paul M, Sudhakar P. Green Synthesis, Characterization, and Antimicrobial Evaluation of Silver Nanoparticles Using Azadirachta indica (Neem) Leaf Extract: A Sustainable Approach to Nanotechnology. International Journal of Science and Research (IJSR). 2026:975-978.
18. Khalil MMH, Ismail EH, El-Baghdady KZ, Mohamed D. Green synthesis of silver nanoparticles using olive leaf extract and its antibacterial activity. Arabian Journal of Chemistry. 2014;7(6):1131-1139.
19. Dhir R, Chauhan S, Subham P, Kumar S, Sharma P, Shidiki A, et al. Plant-mediated synthesis of silver nanoparticles: unlocking their pharmacological potential–a comprehensive review. Frontiers in Bioengineering and Biotechnology. 2024;11.
20. Hosny S, Gaber GA, Ragab MS, Ragheb MA, Anter M, Mohamed LZ. A Comprehensive Review of Silver Nanoparticles (AgNPs): Synthesis Strategies, Toxicity Concerns, Biomedical Applications, AI-Driven Advancements, Challenges, and Future Perspectives. Arabian Journal for Science and Engineering. 2025.
21. Mittal AK, Chisti Y, Banerjee UC. Synthesis of metallic nanoparticles using plant extracts. Biotechnol Adv. 2013;31(2):346-356.
22. Kedzierski L, Sakthianandeswaren A, Curtis J, Andrews P, Junk P, Kedzierska K. Leishmaniasis: Current Treatment and Prospects for New Drugs and Vaccines. Curr Med Chem. 2009;16(5):599-614.
23. Tracking Universal Health Coverage: 2023 Global Monitoring Report: World Bank; 2023 2023/09/18.
24. Li S, Qiu T, Zhao N, Liu M, He X, Wang X, et al. Global burden of leishmaniasis, 1990–2021: systematic analysis of the global burden of disease study. International Journal for Equity in Health. 2025;24(1).
25. Melby PC, Tryon VV, Chandrasekar B, Freeman GL. Cloning of Syrian Hamster (Mesocricetus auratus) Cytokine cDNAs and Analysis of Cytokine mRNA Expression in Experimental Visceral Leishmaniasis. Infection and Immunity. 1998;66(5):2135-2142.
26. Sundar S, Chakravarty J. Recent Advances in the Treatment of Leishmaniasis. Pediatr Infect Dis J. 2024;43(9):e310-e313.
27. Nsanzabana C, Rosenthal PJ. In Vitro Activity of Antiretroviral Drugs against Plasmodium falciparum. Antimicrobial Agents and Chemotherapy. 2011;55(11):5073-5077.
28. Elikaee S, Taylor J, Carter N, Dwarka K, Roberts S. Biogenically Synthesized Nanoparticles as Emerging Therapeutics for Leishmaniasis: A Review of Recent Advances and Potential Promises. International Journal of Nanomedicine. 2025;Volume 20:12467-12484.
29. Malek A. Successful Outcomes of Severe COVID-19 in Patient with Chronic Lymphocytic Leukemia: Diagnostic Challenges in Immunocompromised Hosts. Mediterr J Hematol Infect Dis. 2020;12(1):e2020044.
30. Dourado D, Silva Medeiros T, do Nascimento Alencar É, Matos Sales E, Formiga FR. Curcumin-loaded nanostructured systems for treatment of leishmaniasis: a review. Beilstein Journal of Nanotechnology. 2024;15:37-50.
31. Hajipour MJ, Fromm KM, Akbar Ashkarran A, Jimenez de

Aberasturi D, Larramendi IRd, Rojo T, et al. Antibacterial properties of nanoparticles. Trends Biotechnol. 2012;30(10):499-511.
32. ElSawy AM, Attia NF, Mohamed HI, Mohsen M, Talaat MH. Innovative coating based on graphene and their decorated nanoparticles for medical stent applications. Materials Science and Engineering: C. 2019;96:708-715.
33. Kundu N. Copper Nanoparticles as Emerging Anticancer Agents: Mechanistic Insights, Therapeutic Potential, and Future Perspectives. International Journal of Research Publication and Reviews. 2025;6(5):7912-7920.
34. Valiallahi A, Vazifeh Z, Gatabi ZR, Davoudi M, Gatabi IR. PLGA Nanoparticles as New Drug Delivery Systems in Leishmaniasis Chemotherapy: A Review of Current Practices. Curr Med Chem. 2024;31(39):6371-6392.
35. Chang EH. Targeted nanodelivery: materializing the potential of nanomedicine for cancer treatment and diagnosis. Nanomed Nanotechnol Biol Med. 2006;2(4):274.